Supplementary Information (SI) for New Journal of Chemistry.

Valorizing Coal Gasification Fine Slag through a 'Division of Labor' Mechanism for Sustainable Soil Remediation

Gang Yuan, Yujie Dai, Ningning Li, Facun Jiao, Hanxu Li, Chengli Wu*

School of Chemical Engineering, Anhui University of Science and Technology, Huainan 232001, P. R. China

Corresponding Author

* gangyuan@aust.edu.cn

Table S1 Basic characteristics of the soil and CGFS used in this study

	Proximate analysis				Ultimate analysis				
	Moisture	Ash	Volatile	Fixed Carbon	C	H	O	N	S
soil	4.85	89.36	5.55	0.24	1.01	0	4.77	0	0.012
CGFS	29.54	35.07	2.59	32.79	35.03	0	0.34	0	0.012

Table S2 XRF analysis of the soil and CGFS used in this study

Sample	SiO_2	Al_2O_3	Fe_2O_3
Soil	68.57%	16.24%	5.18%
20CGFS	64.85%	18.08%	5.95%
50CGFS	62.20%	19.16%	5.87%
80CGFS	54.44%	22.03%	7.61%
CGFS	42.90%	26.30%	13.76%

Table S3 Main properties of CGFS

	pH	Bulk density(g/cm^3)	Carbon content(g/kg)	SWA(%)
CGFS	8.0	0.54	350.3	62.9

Table S4 Pore structure parameters of Soil and CGFS

	SSA(m^2/g)	total pore volume (cm^3/g)	t-Plot micropore volume\ (cm^3/g)	mesopore volume (cm^3/g)	average pore diameter (nm)
Soil	29.9815	0.035723	0.001750	0.033973	6.6402
50CGFS	112.4545	0.133274	0.006276	0.126998	6.6695
CGFS	191.5275	0.219624	0.012766	0.206858	6.0641

Table S5 EC values of pure an CGFS amended soil before and after planting (μS/cm)

	CGFS Application rate			
	0%	20%	50%	80%
Before planting	154±3	283±4	407±3	642±6
After planting	306±6	347±5	323±5	487±4

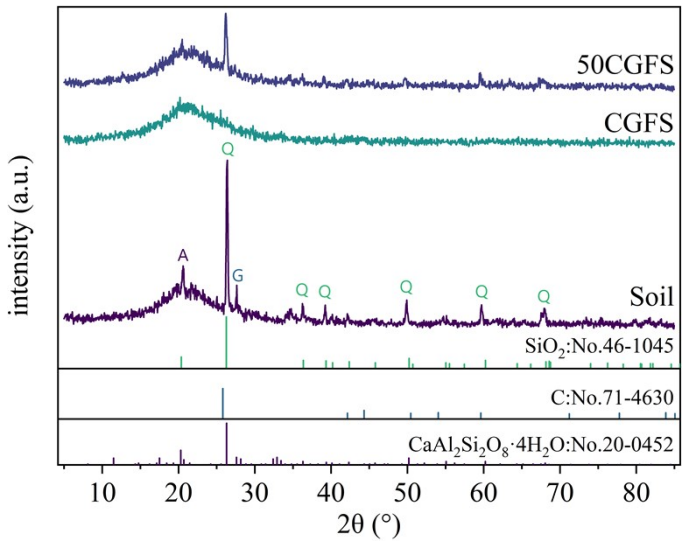

Fig. S1. XRD patterns of pristine soil, raw CGFS, and 50% CGFS-amended soil before and after tomato cultivation. Peaks labeled: Q = quartz (SiO_2), G = graphite, A = albite ($CaAl_2Si_2O_8 \cdot 4H_2O$).

XRD analysis (Fig. S1) revealed that CGFS is an amorphous, multi-phase material composed of quartz (SiO_2), graphite (G), and albite ($CaAl_2Si_2O_8 \cdot 4H_2O$). This combination of a high surface area, mesoporous structure, and mineralogical complexity endows CGFS with an intrinsic ion exchange capacity that far surpasses that of conventional, inert amendments.

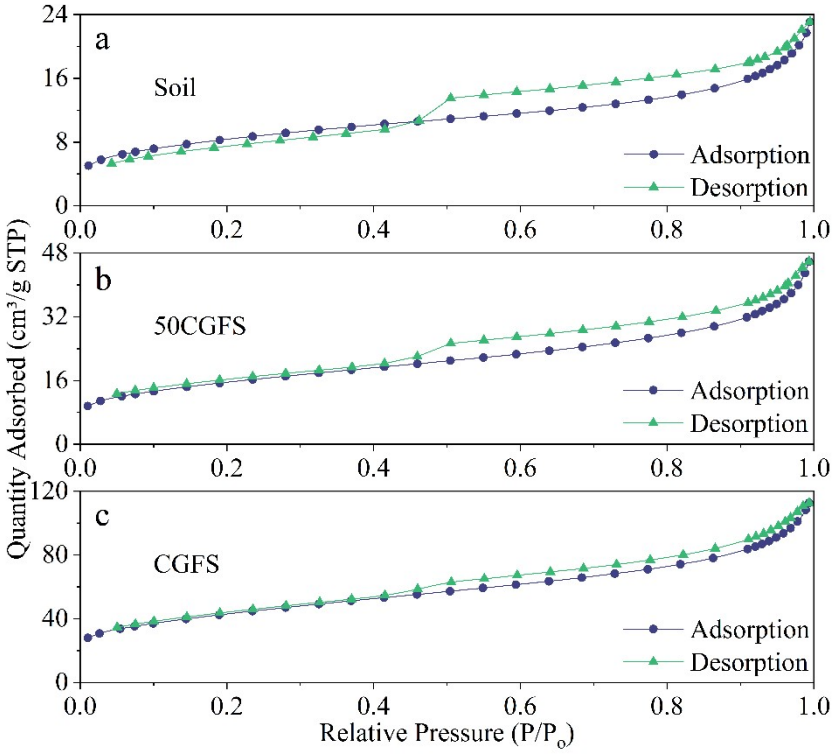

Fig. S2 N_2-adsorption/desorption isotherms of (a) Soil, (b) 50% wt. incorporation of CGFS, and (c) CGFS

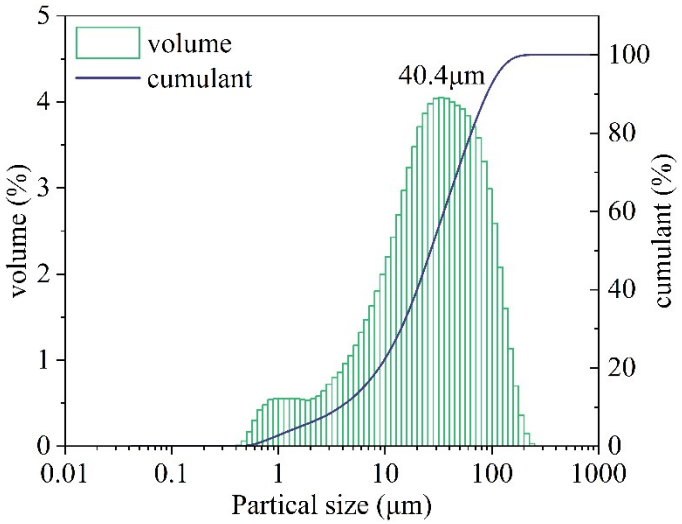

Fig. S3 Particle size distribution of CGFS

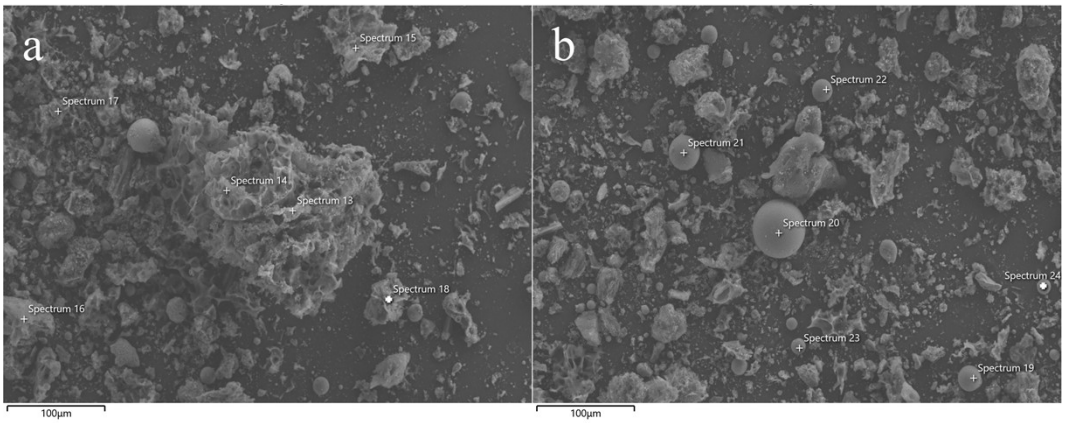

Fig. S4 SEM images of 50-CGFS after planting (a) flocculent aggregates and (b) spherical particles with corresponding elemental point EDX analysis

Table S6 Atom percent of Cd and Pb of CGFS on the irregularly-shaped particle

At%	S13	S14	S15	S16	S17	S18
Cd	0	0.02	0	0.01	0.01	0
Pb	0.02	0.04	0.02	0.03	0.01	0.01

Table S7 Atom percent of Cd and Pb of CGFS on the spherical particle

At%	S19	S20	S21	S22	S23	S24
Cd	0.07	0	0.09	0.03	0	0.04
Pb	0.03	0.02	0	0.01	0.01	0.02

Fig. S4 presents SEM-EDS images of CGFS after the planting cycle, revealing two primary morphologies: flocculent carbonaceous structures (Fig. S4a) and spherical aluminosilicate compounds (Fig. S4b). Point analyses were conducted on both, with spots S13-S18 located on the irregular particles and spots S19-S24 on the spherical particles. The elemental composition (Tables S6-7) revealed significant differences and a clear pattern of distribution. The spots on the irregular particles (S13-S18) had a consistent composition dominated by carbon (86.10%), oxygen (11.73%), and a small amount of silicon (0.83%). These locations exhibited a low atomic percentage of Cd but a high percentage of Pb. In contrast, the spots on the spherical particles (S19-S24) were primarily composed of oxygen (57.96%), carbon (18.31%), and silicon (11.54%), and displayed the opposite trend with a high atomic percentage of Cd and a low percentage of Pb. These results indicate that the spherical structures in CGFS are mainly composed of silicon and oxygen, while the flocculent structures are carbonaceous. Furthermore, Cd tends to be immobilized on silicate-oxygen spherical surfaces, whereas Pb preferentially binds to carbon-rich structures.